Atmos. Chem. Phys. Discuss., https://doi.org/10.5194/acp-2018-918
Manuscript under review for journal Atmos. Chem. Phys.
Discussion started: 1 October 2018

Atmospheric Chemistry and Physics Discussions

Consequences of dynamic and timing properties of new aerosol particle formation and consecutive growth events

Imre Salma and Zoltán Németh

Institute of Chemistry, Eötvös University, H-1518 Budapest, P.O. Box 32, Hungary

Correspondence to: Imre Salma (salma@chem.elte.hu)

Abstract. Dynamic properties, i.e. particle formation rate J_6 and particle diameter growth rate GR_{10}, and timing properties, i.e. starting time (t_1) and duration time interval (Δt) of 247 quantifiable (class 1A) atmospheric new particle formation (NPF) and consecutive particle diameter growth events identified in the city centre and near-city background of Budapest over 6 full measurement years together with related gas-phase H_2SO_4 proxy, condensation sink (CS) of vapours, basic meteorological data and concentrations of criteria pollutant gases were derived, evaluated, discussed and interpreted. In the city centre, nucleation ordinarily starts at 09:15 UTC+1, and it is maintained for approximately 3 h. The NPF and growth events produce 4.6 aerosol particles with a diameter of 6 nm in 1 cm^3 of air in 1 s, and cause the particles with a diameter of 10 nm to grow with a typical rate of 7.3 nm h^{-1}. Nucleation starts approximately 1 h earlier in the near-city background, it shows substantially smaller J_6 (with a median of 2.0 cm^{-3} s^{-1}) and GR_{10} values (with a median of 5.0 nm h^{-1}), while the duration of nucleation is similar to that in the centre. Monthly distributions of the dynamic properties and daily maximum H_2SO_4 proxy do not follow the mean monthly pattern of the event occurrence frequency. The factors that control the event occurrence and that govern the intensity of particle formation and growth are not directly linked. Condensing atmospheric chemical species and/or their processes in the city centre seem to contribute equally to new particle formation and particle growth. In the near-city background, however, chemical compounds available and their processes power particle growth more than particle formation. There is a minimum growth rate of approximately 1.8 nm h^{-1} that is required for nucleated particles to reach the lower end of the diameter interval measured (6 nm) under the actual/local conditions. Monthly distributions and relationships among the properties mentioned provided several indirect evidence that chemical species other than H_2SO_4 largely influence the particle growth and possibly atmospheric NPF process as well. The J_6, GR_{10} and Δt can be described by log-normal distribution. Most of the extreme dynamic properties could not be explained by H_2SO_4 proxy, CS, meteorological data or pollutant gas concentrations. Approximately 40% of the NPF and

Atmos. Chem. Phys. Discuss., https://doi.org/10.5194/acp-2018-918
Manuscript under review for journal Atmos. Chem. Phys.
Discussion started: 1 October 2018

Atmospheric Chemistry and Physics Discussions

growth events exhibited broad beginning, which can be an urban feature. For 9% of all cases, it was feasible to calculate 2 separate sets of dynamic properties. The later onset frequently shows more intensive particle formation and growth than the first onset by a typical factor of approximately 1.4. The first event is of regional type, while the second event, superimposed on the first, is often associated with sub-regional, thus urban NPF and growth process.

1 Introduction

Molecules and molecular fragments in the air collide randomly, and can form electrically neutral or charged clusters. Most clusters decompose shortly. Chemical stabilising interactions among certain components within a cluster can enhance its lifetime, during which it can grow further by additional molecular collisions through some distinguishable size regimes (Kulmala et al., 2014). If the diameter of these clusters reaches a critical value of 1.5±0.3 nm (Kulmala et al., 2013), they become thermodynamically stable, and their further growth turns into a spontaneous process. Supersaturation is a necessary atmospheric condition for this principal conversion. It is virtually a phase transition, which takes place in a dispersed manner in the atmosphere, so it generates an aerosol system. The newly formed particles grow further by condensation to larger particles in most cases due to the existing supersaturation. Photochemical oxidation products such as H_2SO_4 (Sipilä et al., 2010), extremely low-volatile organic compounds (ELVOCs, Ehn et al., 2014; Jokinen et al., 2015) and highly oxygenated molecules (HOMs, Bianchi et al., 2016; Kirkby et al., 2016; Tröstl et al., 2016) together with H_2O vapour, NH_3 (Kirkby et al., 2011), amines (Almeida et al., 2013), other oxidation products of volatile organic compounds (VOCs; Metzger et al., 2010; Schobesberger et al., 2013; Riccobono et al., 2014) and NO_2 can play an important role in both the formation and growth. The VOCs include compounds of anthropogenic and biogenic origin mainly isoprenoids such as α-pinene (Kirkby et al., 2016). In some specific coastal regions, iodine oxides produced from marine biota are involved (O'Dowd et al., 2002). Atmospheric concentration of these key compounds at a level that is smaller typically by 12–14 orders of magnitude than the concentration of air molecules is already sufficient for the phenomenon (Kulmala et al., 2014). Relative importance of the organics increases with particle size (Riipinen et al., 2011; Ehn et al., 2014), and their supersaturation is maintained by fast gas-phase autooxidation chemical reactions of VOCs (Crounse et al., 2013). The overall phenomenon is ordinarily confined in time for 1 day or so, and, therefore, it can be regarded as an event in time, and is referred as new aerosol particle formation (NPF) and consecutive particle growth event.

Such events appear to take place almost everywhere in the world and anytime (Kulmala et al., 2004; Nieminen et al., 2018). Their occurrence frequency and, more importantly, their contribution to particle number concentrations were found to be substantial or determinant in the global troposphere (Spracklen et al., 2006; Kulmala et al., 2014). Moreover, their contribution to the number of cloud condensation nuclei (CCN) can be 50% or even more (Makkonen et al., 2009; Merikanto et al, 2009; Sihto et al., 2011), which links the events to climate system, and emphasizes their global relevance (Kerminen et al., 2012; Carslaw et al., 2013; Makkonen et al., 2012; Gordon et al., 2016). New particle formation and growth events were proved to be common in polluted air of large cities as well with a typical relative occurrence frequency between 10% and 30% (Woo et al., 2001; Baltensperger et al., 2002; Alam, et al., 2003; Wehner et al., 2004; Salma et al., 2011; Dall'Osto et al., 2013; Xiao et al., 2015; Zhang et al., 2015; Kulmala et al., 2017, Nieminen et al., 2018). The coupling and relationships between regional and urban (sub-regional) NPF was demonstrated at least under favourable orographic conditions (Salma et al., 2016b). New particle formation can increase the existing particle number concentrations in city centres by a factor of approximately 2 on nucleation days, while it can produce approximately 28% of ultrafine (UF) particles on a longer (e.g. annual) time scale (Salma et al., 2017). Particle concentrations from NPF are also important when compared to the (primary) particles emitted by their dominant source in cities, namely by road vehicles with internal combustion engines (Paasonen et al., 2016). These jointly imply that particles from NPF and growth events in cities can influence not only the urban climate but can contribute to the public's excess health risk from particle number exposures (Oberdörster et al., 2005; Braakhuis et al., 2014; Salma et al., 2015), and, furthermore, could be linked to the role of human actions in all these effects.

In spite of these potentials, conclusive interpretation of the data obtained and results derived specifically for cities remained hindered so far. Several-year long semi-continuous critically evaluated and coherent data sets are require for this purpose, which have been generated gradually. As part of this international progress, investigations dedicated to urban NPF and growth events in Budapest have been going on since November 2008. Measurements for 5 full years were realised in the city centre at a fixed location, 1 full year was devoted to measurements in a near-city background environment, and some other measurements were accomplished in different urban microenvironments for time intervals of a few months. The main objectives of this study are to determine, present and analyse the dynamic properties, i.e.

particle formation rate and particle diameter growth rate, timing properties, i.e. starting time and duration time interval of nucleation process of NPF and growth events together with the major sources and sink of condensing vapours, basic meteorological data and criteria pollutant gases for 6 years, to investigate and interpret their relationships, to discuss their monthly distributions, to evaluate and detect some of their features specific for urban atmospheric environments, and to demonstrate some specific urban influence on the determination of these properties. These quantities and relationships are of basic importance in many atmospheric processes for several reasons, and some of them are also discussed.

2 Experimental methods

The measurements took place at two urban locations in Budapest, Hungary. Most measurements were realised at the Budapest platform for Aerosol Research and Training (BpART) facility (N 47° 28' 29.9", E 19° 3' 44.6", 115 m above mean see level (a.s.l.; Salma et al., 2016a). This site represents a well-mixed, average atmospheric environment for the city centre. The other location was situated at the NW border of Budapest in a wooded area of the Konkoly Astronomical Observatory of the Hungarian Academy of Sciences (N 47° 30' 00.0", E 18° 57' 46.8", 478 m a.s.l.). This site characterises the air masses entering the city since the prevailing wind direction in the area is NW. The measurements were accomplished for 6 full-year long time intervals, i.e. from 03–11–2008 to 02–11–2009, from 19–01–2012 to 18–01–2013, from 13–11–2013 to 12–11–2014, from 13–11–2014 to 12–11–2015, from 13–11–2015 to 12–11–2016 and from 28–01–2017 to 27–01–2018. In the measurement year 2012–2013, the instruments were set up in the near-city background, while in all other years, they were installed in the city centre. Local time (LT=UTC+1 or daylight saving time, UTC+2) was chosen as the time base of the data unless otherwise indicated because the daily activity time pattern of inhabitants substantially influences the atmospheric processes in cities (Salma et al., 2014).

The main measuring system was a flow-switching type differential mobility particle sizer (DMPS). It consists of a radioactive (^{60}Ni) bipolar charger, a Nafion semi-permeable membrane dryer, a 28-cm long Vienna-type differential mobility analyser and a butanol-based condensation particle counter (TSI, model CPC3775). The sample flow was 2.0 L min^{-1} in the high-flow mode, and 0.31 L min^{-1} in the low-flow mode with sheath air flow rates 10 times larger than for the sample flows. The DMPS measures particle number concentrations in an electrical mobility diameter range from 6 to 1000 nm in the dry state of particles (with a relative

humidity of RH<30%) in 30 channels, which finally yields 27 channels after averaging 3 overlapping channels when joining the data for the 2 flow modes. The time resolution of the measurements was approximately 10 min till 18–01–2013, and 8 min from 13–11–2013 (after a planned update of the DMPS system). There was no upper size cut-off inlet applied to the sampling line, and a weather shield and insect net were only attached. The sampling inlet was installed at a height of 12.5 m above the street level in the city centre, and of approximately 1.7 m in the near-city background. The measurements were performed according to the international technical standard (Wiedensohler et al., 2012). The availability of the DMPS data over 1-year long time intervals are summarised in Table 1. Synoptic meteorological data for air temperature (*T*), RH, wind speed (WS) and wind direction (WD) were obtained from a measurement station of the Hungarian Meteorological Service (HMS, no. 12843) by standardised methods with a time resolution of 1 h. Global solar radiation (GRad) data were measured by the HMS at a distance of 10 km in E direction with a time resolution of 1 h. Meteorological data were available in >90% of the possible cases in each year. Concentrations of SO_2, O_3, NO_x and CO were obtained from measurement stations of the National Air Quality Network in Budapest (in a distance of 4.5 km from the urban site, and of 6.9 km from the near-city background site) located in the upwind prevailing direction from the measurement sites. They are measured by UV fluorescence (Ysselbach 43C), UV absorption (Ysselbach 49C), chemiluminescence (Thermo 42C) and IR absorption methods (Thermo 48i), respectively with a time resolution of 1 h. The concentration data were available in >85% of the yearly time intervals. It is worth mentioning that concentration of SO_2 in the Budapest area is ordinarily distributed without larger spatial (and temporal) differences (Salma et al., 2011). For the present study, this was actually proved by evaluating the concentration ratios from two different municipal station which were located in 2 different directions with an angle between them of 60° in the closest distance from the BpART. The mean SO_2 concentration ratio and standard deviation (SD) for the 2 stations were 81±20% over the 5-year long measurement time interval, which appears to lay within the experimental uncertainty. The assumption can be justified indirectly by a conclusion on the monthly distribution of SO_2 concentration in Sect. 4.2.

3 Data treatment

The measured DMPS data were evaluated according to the procedure protocol recommended by Kulmala et al. (2012) with some refinements that are related mainly to urban features (see Sect. 3.1). Particle number concentrations in the diameter ranges from 6 to 1000 nm (*N*), from

6 to 25 nm ($N_{6–25}$) and from 6 to 100 nm ($N_{6–100}$ or UF particles) were calculated from the measured and inverted DMPS concentrations. Particle number size distribution surface plots showing jointly the variation in particle diameter and particle number concentration density in time were also generated. Identification and classification of NPF and growth events was accomplished on these surface plots (Dal Maso et al., 2005; refined in Németh et al., 2018 for urban sites) on a daily basis into the following main classes: NPF event days, non-event days, days with undefined character, and days with missing data (for more than 4 h during the midday). Relative occurrence frequency of events was determined for each month and year as the ratio of the number of event days to the total number of relevant (i.e. all–missing) days. A subset of events with uninterrupted evolution in time, which are called quantifiable (class 1A) events, were further distinguished because the time evolution of their size distribution functions were utilised to determine the dynamic and timing properties with good accuracy and reliability.

3.1 Dynamic and timing properties

Growth rate (GR) of nucleation-mode particles was calculated by mode-fitting method (Kulmala et al., 2012). Particle number median mobility diameter (NMMD) of the nucleation mode were obtained from fitting the individual size distributions by DoFit algorithm (Hussein et al., 2004). The growth rate was determined as the slope of the linear line fitted to the time series of the NMMD data within a time interval around a diameter d, where the dependence could be satisfactorily approximated by linear fit. Since the nucleation mode was mostly estimated by $N_{6–25}$ in the calculations of the formation rate (see below), and since the median of the related diameter interval (from 6 to 25 nm) is close to d=10 nm, GRs for particles with a diameter of 10 nm were determined (GR_{10}). This type of GR can be interpreted as an average GR as far as the given particle diameter range is concerned, but it actually expresses the beginning of the growth process only, which may have considerable effects on the formation rate calculations in specific cases (see later).

Time evolution of an aerosol population is described by the general dynamic equation which was rearranged, simplified and approximated by several quantities (Kulmala et al., 2001; Dal Maso et al., 2002; Kulmala et al., 2012; Cai and Jiang, 2017) to express the formation rate J_6 of particles with the smallest detected diameter of d_{min}=6 nm in a form actually utilised in the present evaluation as

Atmos. Chem. Phys. Discuss., https://doi.org/10.5194/acp-2018-918
Manuscript under review for journal Atmos. Chem. Phys.
Discussion started: 1 October 2018

Atmospheric Chemistry and Physics Discussions

$$J_6 = \frac{\mathrm{d}N_{6\text{-}25}}{\mathrm{d}t} + \mathrm{CoagS}_{10} N_{6\text{-}25} + \frac{\mathrm{GR}_{10}}{(25-6)} N_{6\text{-}25} - \frac{\mathrm{d}N_{\mathrm{Ai},<25}}{\mathrm{d}t}. \quad (1)$$

The first term on the right side of Eq. 1 expresses the concentration increment. The particle number concentration in the size range from 6 to 25 nm ($N_{6–25}$) was selected to approximate the nucleation-mode particles $N_{nuc} \approx N_{6–25}$. This is a usual and reasonable choice because it was proved to be advantageous and effective way in handling fluctuating data sets since $N_{6–25}$ often exhibits less sensitivity and smaller scatter in time than the fitted area of the nucleation mode. It is implicitly assumed that the intensity of the NPF is constant for a certain time interval, and, therefore, $\mathrm{d}N_{6–25}/\mathrm{d}t$ can be determined as the slope of the linear function of $N_{6–25}$ versus time t within an interval where the dependence could be satisfactorily approximated by linear fit. A limitation of the relatively wide size range (6–25 nm) selected can be manifested by disturbances from primary particles in particular in urban environments. This is taken into account by the last term of Eq. 1, and is discussed later. The second term on the right side of Eq. 1 expresses the loss of particles due to coagulation scavenging (due to pre-existing larger particles). The coagulation scavenging efficiency for particles with a diameter of 10 nm (CoagS_{10}) was selected to approximate the mean coagulation efficiency of nucleation-mode particles (CoagS_{nuc}). This diameter was chosen by considering the median of the related diameter range, which was discussed above for GR. The coagulation efficiency was calculated from classical aerosol mechanics with adopting a mass accommodation coefficient of 1 and utilizing the Fuchs' transition-regime correction factor separately for all the size channels belonging to the selected size range (Kulmala et al., 2001; Dal Maso et al., 2005; Kulmala et al., 2013) by using the computation scripts of the University of Helsinki. Self-coagulation within the nucleation mode was neglected due to its limited concentration. Hygroscopic growth of particles was not considered since this depends on chemical composition of particles, which is unknown but expected to change substantially in time. The third term on the right side of Eq. 1 expresses the particle growth out of the considered size range by condensation of vapours. The GR_{10} was selected to approximate a representative value at the median of the particle diameter range considered (Vuollekoski et al., 2012). It is implicitly assumed that GR_{10} can be regarded to be constant over the time interval of interest. Nevertheless, the diameter growth of nucleation-mode particles in time is occasionally strongly limited (Fig. S1a). In these specific cases, the mean relative area of the nucleation mode below 25 nm was determined by fitting the individual size distributions around the time of the maximum nucleation-mode NMMD, and the ratios were averaged. The correction in form of the mean relative area was adopted as a

Atmos. Chem. Phys. Discuss., https://doi.org/10.5194/acp-2018-918
Manuscript under review for journal Atmos. Chem. Phys.
Discussion started: 1 October 2018

Atmospheric Chemistry and Physics Discussions

multiplication factor for the growth out term in Eq. 1. On a very few days, the particle growth was followed by a decrease in nucleation-mode NMMD (Salma et al., 2016a). In these cases, the shrinkage rate (with a formal $GR_{10}<0$) was derived and adopted. The fourth term on the right side of Eq. 1 expresses the contribution of (high-temperature) emission sources, usually vehicular road traffic (Paasonen et al., 2016; Salma et al., 2017) to the $N_{6–25}$, which can provisionally disturb the assumption of $N_{nuc}\approx N_{6–25}$. A typical example of such a situation is shown in Fig. S1b from 10:09 to 12:23 LT. In these specific cases, the contribution of primary emissions was estimated from the slope of the time series of the fitted peak area of the Aitken mode below $d<25$ nm ($N_{Ai,<25}$) in the time region of interest. Reliable separation of the nucleation and Aitken modes from each other was hindered or was not possible for a few individual size distributions due to overlapping modes and scatter in the concentration data, and these individual Aitken-mode areas were excluded from or skipped in the time series. Relative contributions of the concentration increment, coagulation loss and growth out from the diameter interval – which were significant in all calculations – to J_6 are decreasing in this order with mean values of 71%, 17% and 12%, respectively (Table S1).

The formation and growth rates for the measurement years of 2008–2009 and 2012–2013 were obtained earlier by a slightly different way and neglecting the urban features (Salma et al., 2011, 2016b). To obtain consistent data sets, the dynamic properties for these 2 years were re-evaluated now by adopting the refinements described above and implementing the experience gained over the years. The mean new-to-old rate ratios with SDs for the GR_{10} and J_6 were 1.06±0.32 and 1.23±0.37, respectively in the city centre (2008–2009) and 1.04±0.21 and 1.20±0.35, respectively in the near-city background (2012–2013). The re-calculation yielded non-negligible improvements for the mean formation rates. Some individual formation and growth rates, in particular the smaller values, were substantially impacted.

The assumption and estimations above usually represent a reasonable approximation to reality. The $N_{6–25}$ is derived from the experimental data in a straightforward way, the GR_{10} and the corrections for primary particles and limited particle growth depend on the quality of the size distribution fitting program as well, while the $CoagS_{10}$ is determined by using a theoretical model. The resulting accuracies of the dynamic properties, in particular of J_6, look rather complicated, and depend on the spatial heterogeneity in the air masses measured particularly for the observations performed at a fixed site, size and time resolution of the concentrations measured, diameter range of the size distributions, fluctuations in the experimental data,

selection of the particle diameter channels (interval), choice of the time interval of interest (for linear fits), sensitivity of the models to the uncertainties (Vuollekoski et al., 2012), and also on the extent of the validity of the assumptions applied – particularly under highly polluted conditions (Cai and Jiang, 2017). The situation is further complicated with the fact that the dynamic (and also the timing) properties are connected to each other. Finally, it is important to recognise that some NPF and growth curves on the surface plots have rather broad starting time interval (Fig. S1a and S1c). They occur in a considerable abundance in cities, e.g. in 40% of all quantifiable events in Budapest (Sect. 4.4). This may yield badly defined or composite dynamic properties, whose uncertainty can have principle limitations overwhelming the experimental and model uncertainties.

Timing properties of NPF and growth events are increasingly recognised, and they can provide very valuable information even if they are estimated indirectly from the observed diameter interval >1.5 nm (Sect. 1). The earliest estimated time of the beginning of a nucleation (t_1) and the latest estimated time of the beginning of a nucleation (t_2) were derived by a comparative method (Németh and Salma, 2014) based on the variation in the content of the first size channel of the DMPS system. Both time parameters includes a time shift that accounts for the particle growth from the stable neutral cluster mode at approximately 2 nm to the smallest detectable diameter limit of the DMPS systems (6 nm in our case) by adopting the GR value in the size window nearest to it in size space. The difference $\Delta t=t_2-t_1$ was considered as the duration time interval of the nucleation process. It represents the time interval during which new aerosol particles are generated in the air. The uncertainty of the timing parameters is regarded to be around 30 min under ordinary NPF and growth situations.

3.2 Sources and sink

Gas-phase H_2SO_4 was not measured in the campaigns, and its relative effect was estimated by its proximity measure (proxy) containing both the major source and sink terms under steady-state conditions according to Petäjä et al. (2009). It was calculated for radiations >10 W m^{-2}. In principle, it is possible to convert the H_2SO_4 proxy values to H_2SO_4 concentrations by an empirical scaling factor of $k=1.4\times10^{-7}\times\mathrm{GRad}^{-0.70}$, where GRad is expressed in a unit of W m^{-2} (Petäjä et al., 2009). The factor was, however, derived for a remote boreal site, and, therefore, we usually prefer not to perform the conversion since urban areas are expected to differ from the boreal regions, and adopting the factor could distort the dynamic relationships or time trends

303 investigated. The conversion was applied only to estimate the order of average H_2SO_4
304 atmospheric concentration levels. The results derived by utilising the proxy are subject to larger
305 uncertainties than in other cases because of these limitations, but they may indicated gross
306 tendencies.
307
308 Condensation sink for vapour molecules onto the surface of existing aerosol particles was
309 computed for discrete size distributions as described in earlier papers (Kulmala et al., 2001; Dal
310 Maso et al., 2002, 2005) and summarised by Kulmala et al. (2013). The equilibrium vapour
311 pressure of the condensing species was assumed implicitly to be negligible at the surface of the
312 particles, so similar to sulfuric acid. Dry particle diameters were considered in the calculations.
313
314 **4 Results and discussion**
315
316 Annual median particle number concentrations based on the individual data in the near-city
317 background in 2012–2013, and in the city centre for the separate measurement years of 2008–
318 2009, 2013–2014, 2014–2015, 2015–2016 and 2017–2018 were 3.4×10^3, and 11.5×10^3,
319 9.7×10^3, 9.3×10^3, 7.5×10^3 and 10.6×10^3 cm^{-3}, respectively, which indicate some overall
320 decreasing trend in the city centre. There was no obvious pattern in the distribution of monthly
321 median particle number concentrations. The mean UF/*N* ratio with SD for the same
322 measurement time intervals were 67±14%, and 79±6%, 75±10%, 75±11%, 76±11% and
323 80±10%, respectively. The values correspond to ordinary urban atmospheric environments in
324 Europe (Putaud et al., 2010). An overview on the number of classified days separately for the
325 1-year long measurement time intervals is given in Table 1. The availability of the daily size
326 distribution surface plots with respect to all days ensures that the data are representative on
327 yearly and monthly time scales, except for 08 and 09–2015, when there were missing days in
328 larger ratios. The number of quantifiable event days (248 cases) is also considerable, which
329 establishes to arrive at firm conclusion on the NPF and growth events as well.
330

Atmos. Chem. Phys. Discuss., https://doi.org/10.5194/acp-2018-918
Manuscript under review for journal Atmos. Chem. Phys.
Discussion started: 1 October 2018

Atmospheric Chemistry and Physics Discussions

Table 1. Number of days with new aerosol particle formation and growth event, quantifiable (class 1A) event days, non-event days, undefined days, missing days and the coverage of relevant days with respect to all days in the near-city background and city centre separately for the 1-year long measurement time intervals.

Environment	Background	Centre				
Time interval	2012–2013	2008–2009	2013–2014	2014–2015	2015–2016	2017–2018
Event days	96	83	72	81	35	83
Quantifiable days	43	31	48	56	18	52
Undefined days	19	34	24	25	8	23
Non-event days	231	229	267	240	226	257
Coverage (%)	95	95	99	95	73	99
Missing days	20	19	2	19	97	2

It was previously shown that the NPF and growth events observed in the city centre and its background ordinarily happen above a larger territory or region (Salma et al., 2011; Németh and Salma, 2014), and they are linked to each other (Salma et al., 2016b). From the point of the occurrence frequency distribution, they could, therefore, be evaluated jointly in the first approximation. An overall monthly mean relative occurrence frequency of nucleation days derived for all 6 measurement years is shown in Fig. 1. The annual mean frequency with SD was 22±5%, which is considerable and is in line with other urban sites (Sect. 1). The monthly mean frequency has a temporal variation, which can be characterised by a noteworthy pattern. The mean monthly dependency exhibits an absolute and a local minimum in January (5.6%) and August (21%), respectively, and an absolute and a local maximum in April (40%), and September (31%), respectively. Nevertheless, the SDs of the monthly (and annual) means indicate prominent variability from year to year. The pattern can be related to multivariate relationships and complex interplay among the influencing factors, which include the air temperature (January is the coldest month, while August is the warmest month in the Carpathian Basin) and enhanced emission of biogenic VOCs in springtime (March–April) and early autumn (September) as well (Salma et al., 2016b).

Atmos. Chem. Phys. Discuss., https://doi.org/10.5194/acp-2018-918
Manuscript under review for journal Atmos. Chem. Phys.
Discussion started: 1 October 2018

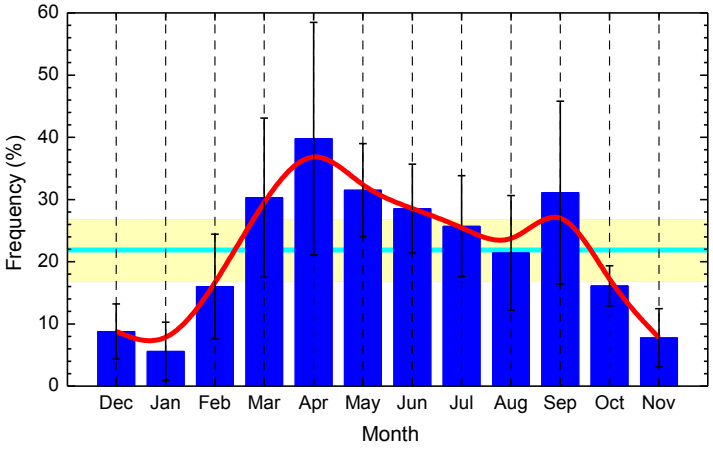

Figure 1. Monthly mean relative occurrence frequency of new aerosol particle formation and consecutive particle diameter growth events with respect to the number of relevant days for the joint 6-year long data set. The error bars show ±1 standard deviation, the horizontal line in cyan indicates the overall annual mean frequency, the yellow bands represent ±1 standard deviation of the annual mean, and the smooth curve in red serves to guide the eye.

The properties and variables studied were derived in full time resolution. They were averaged in several ways for different conditions and for various purposes to obtain typical average descriptive characteristics. In 1 case (31–08–2016), the NPF and growth event could reliable be identified, while the measured absolute particle number concentrations could not be validated due to some experimental troubles, and, therefore, it was left out from the further calculations. Similarly, there were 1 and 4 NPF and growth events with unusually/extraordinarily large dynamic properties in the measurement years 2014–2015 and 2017–2018, respectively. More specifically, 5 individual J_6 data when expressed in a unit of $cm^{-3}\ s^{-1}$ and 1 individual GR_{10} data when given in $nm\ h^{-1}$ were >20 (Table 3). These extremes were left out from the overview statistics to maintain the representativity (they could be influenced by some unknown extra or very local sources) and to fulfil better the basic requirements of correlation analysis. If an event showed a double beginning then the dynamic properties for the first onset were considered in the basic overview since this onset is of regional relevance (Salma et al., 2016b). The extreme dynamic properties and the characteristics for the second onsets were, however, evaluated separately and are discussed in detail and interpreted in Sect. 4.4.

Atmos. Chem. Phys. Discuss., https://doi.org/10.5194/acp-2018-918
Manuscript under review for journal Atmos. Chem. Phys.
Discussion started: 1 October 2018

389 **4.1 Ranges and averages**

390

391 Ranges and averages with SDs of formation rate J_6, growth rate GR_{10}, starting time of
392 nucleation (t_1) and duration time interval of nucleation (Δt) are summarised in Table 2 for
393 separate measurement years and for the joint 5-year long city centre data set. In the city centre,
394 nucleation generally starts at 09:15 UTC+1, and it is typically maintained for approximately 3
395 h. The NPF and growth events ordinarily produce 5.6 new aerosol particles with a diameter of
396 6 nm in 1 cm^3 of air in 1 s, and cause the particles with a diameter of 10 nm to grow with a
397 typical rate of 7.6 nm h^{-1}. The statistics for J_6 and GR_{10} are based on 199 and 203 events,
398 respectively. The corresponding data for the separate years show considerable variability
399 without obvious trends or tendencies. The differences between the years can likely be related
400 to changes in actual atmospheric chemical and physical situations and conditions, and to the
401 resulting modifications in the sensitive balance and delicate coupling among them from a year
402 to year. Spread of the individual data for GR_{10} is smaller than for J_6; the relative SDs for the
403 joint 5-year long city centre data set were 38% and 68%, respectively, while the (external)
404 relative SDs calculated from the annual mean values were 4.2% and 14.0%, respectively. The
405 dynamic properties and t_1 data tend to be smaller in the near-city background than in the city
406 centre. In general, nucleation starts 1 h earlier in the background, and the events typically show
407 significantly smaller J_6 (with a median of 2.0 cm^{-3} s^{-1}) and GR_{10} (with a median of 5.0 nm h^{-1}).
408 Duration of the nucleation is very similar to that in the city centre. All starting times of
409 nucleation were larger than (in a few cases, very close to) the time of the sunrise. This implies
410 that no nocturnal NPF and growth event has been identified in Budapest so far. The particle
411 growth process (the so-called banana curve) could be traced usually for a longer time interval
412 (up to 1.5 d) in the background than in the centre. These conclusions are in line with the ideas
413 on atmospheric nucleation and consecutive particle growth process (e.g. Kulmala et al., 2014;
414 Zhang et al., 2015), and they also confirm some our earlier findings with respect to Budapest
415 and its regional background within the Carpathian Basin achieved with shorter, 2-year long data
416 sets (Salma et al., 2016b).
417

Atmos. Chem. Phys. Discuss., https://doi.org/10.5194/acp-2018-918
Manuscript under review for journal Atmos. Chem. Phys.
Discussion started: 1 October 2018

Atmospheric Chemistry and Physics Discussions

418 **Table 2.** Ranges, averages and standard deviations of aerosol particle formation rate J_6, particle diameter
419 growth rate GR_{10}, starting time (t_1) and duration time interval ($\Delta t=t_2-t_1$) of nucleation process of
420 quantifiable (class 1A) new particle formation and growth events in the near-city background and city
421 centre separately for the 1-year long measurement time intervals and for the joint 5-year long city centre
422 data set.
423

Environment	Background	Centre					
Time interval	2012–2013	2008–2009	2013–2014	2014–2015	2015–2016	2017–2018	All 5 years
Formation rate J_6 (cm^{-3} s^{-1})							
Minimum	0.48	1.47	1.13	0.81	1.19	1.60	0.81
Median	2.0	4.2	3.5	4.4	4.6	6.3	4.6
Maximum	5.6	15.9	17.8	18.0	15.3	17.3	18.0
Mean	2.2	4.7	5.2	5.6	5.0	6.6	5.6
St. deviation	1.3	2.6	3.7	4.2	3.7	3.3	3.8
Growth rate GR_{10} (nm h^{-1})							
Minimum	3.0	3.7	3.1	2.8	3.2	3.3	2.8
Median	5.0	7.6	6.6	6.5	8.0	7.5	7.3
Maximum	9.8	17.4	19.0	18.0	15.5	19.8	19.8
Mean	5.2	7.8	7.2	7.3	7.7	8.0	7.6
St. deviation	1.4	2.6	2.8	3.2	3.0	2.8	2.9
Starting time, t_1 (HH:mm UTC+1)							
Minimum	05:51	07:14	06:44	05:48	07:31	05:57	05:48
Median	08:19	09:26	09:22	08:48	09:45	09:18	09:15
Maximum	11:09	11:38	12:21	11:23	12:45	12:15	12:45
Mean	08:17	09:27	09:25	08:49	10:02	09:24	09:19
St. deviation	01:11	01:05	01:26	01:22	01:23	01:36	01:26
Duration time, Δt (HH:mm)							
Minimum	01:23	00:52	00:42	00:31	01:03	01:26	00:31
Median	03:16	02:36	02:04	03:53	02:31	03:49	02:57
Maximum	06:44	06:04	05:34	07:46	06:05	07:55	07:55
Mean	03:30	02:44	02:14	03:52	02:58	03:57	03:18
St. deviation	01:40	01:11	01:01	01:40	01:47	01:39	01:40

424

425 Ranges and averages with SDs of some related atmospheric properties, namely of mean CS
426 averaged for the time interval from t_1 to t_2, daily maximum gas-phase H_2SO_4 proxy, daily mean
427 T and RH (Table S2), and of daily median concentrations of SO_2 (as the major precursor of gas-
428 phase H_2SO_4), O_3 (as an indicator of photochemical activity), NO_x and CO gases (as indicators
429 of anthropogenic combustion activities and road vehicle emissions) (Table S3) were also
430 derived for quantifiable NPF and growth event days, and are further evaluated. The annual
431 mean CS values exhibited decreasing tendency in the city centre over the years (as can be

expected from the particle number concentrations as well). The individual values remained below approximately 20×10^{-3} s^{-1}, which agrees well with the results of our earlier study (Salma et al., 2016b) according to which the CS suppresses NPF above this level in the Carpathian Basin. Maximum H_2SO_4 proxy values reached substantially higher levels (by a factor of approximately 2) in the near-city background than in the city centre due mainly to the differences in the CS and also [SO_2]. The differences between the 2 sets of proxy data (between the 2 sites) are particularly evident when considering their smallest values. The largest variability in the annual average values were observed for the proxy. A maximum concentration of H_2SO_4 molecules of 10^6–10^7 cm^{-3} were estimated by adopting the scaling factor (Sect. 3.2). The dynamic properties seem to be not very sensitive to air *T*; which displayed quite similar and comparable values over the years and at both sites. This conclusion is likely linked to several temperature-dependent environmental processes simultaneously present in the area which balance the effect of *T*. Some events happened at daily mean temperatures below zero. The daily mean RH and its SD for the city centre and near-city background were 54±11% and 64±12%, respectively. There were events that occurred at RHs as high as 90%. Relationships of the dynamic properties with *T* and RH are also obscured with strong seasonal cycle of these meteorological data and with the fact that air masses arriving to the receptor site in different trajectories are often characterised by the distinct levels of meteorological data. As far as the pollutant gases are concerned, SO_2 showed somewhat smaller daily median values, and O_3 exhibited substantially smaller levels on event days in the city centre than in the near-city background, while concentrations of NO_x and CO were obviously larger in the city than in its close background. The differences can primarily be explained by the intensity and spatial distribution of their major sources and atmospheric chemical reactions, and the joined concentration data resembles typical situations without photochemical smog episodes in cities. There was no obvious decrease in SO_2 concentration during these years in contrast with an earlier decreasing trend from mid-1980s till about 2000. No evident or sensitive effect of atmospheric gases on the dynamic or timing properties could be deduced from the averaged data. This can probably be explained by a dedicated balance between the intensifying and suppressing effects, which were averaged out on a yearly time scale. Relationships on shorter scales are further investigated and discussed in more detail in the following sections.

4.2 Monthly distributions

Distributions of the monthly mean J_6, GR_{10}, daily maximum gas-phase H_2SO_4 proxy, mean CS, daily mean air *T* and RH, and daily median SO_2, O_3, NO_x and CO concentrations for quantifiable

NPF and growth events for the joint 5-year long city centre data sets are shown in Fig. 2. The distributions – eminently for J_6, GR_{10}, H_2SO_4 proxy and SO_2 – do not follow the monthly pattern of the event occurrence frequency at all (cf. Fig. 1). Instead, the J_6, GR_{10} and H_2SO_4 proxy tend to exhibit larger values in summer months, and they temporal changes over the other months are smooth and do not show distinctive features. The elevations are substantial; the estimated maximum level was larger than the baseline by a factor of 2.1 for the J_6, and by a factor of approximately 1.4 for the GR_{10} and H_2SO_4 proxy. The result is in line with other observations according to which the GR exhibits almost exclusively a summer maximum (Nieminen et al., 2018). The intensity of solar radiation at the surface, its seasonal cycling, concentration of atmospheric condensing vapours in different months, biogenic processes and the fact that rate coefficient of many thermal chemical/physicochemical processes in the nature (including GR, Paasonen et al., 2018) increases with T could play an important role in explained the distributions of the dynamic properties, although a more comprehensive study involving chemicals and their photochemistry is required for more detailed explanation. The properties are biased and influenced jointly by the intensity of the solar electromagnetic radiation. Nevertheless, the misalignment between the monthly distributions of occurrence frequency and all the other properties indicates that 1) the event occurrence or its basic causes are not linked with the dynamic properties in a straightforward or linear manner, and 2) gas-phase H_2SO_4 does not seem to be the controlling factor of NPF occurrence in the Carpathian Basin including Budapest. The mean J_6, GR_{10} and H_2SO_4 proxy data still have considerable uncertainty, which makes their interpretation not yet completely conclusive. The uncertainties are influenced by the inherent fluctuations in the data sets, number of the individual data available for different properties and months, variations in other or unknown relevant environmental conditions, and by their variability from a year to year. The resulting uncertainties are expected to decrease with the length of the available data sets, which emphasized the need for continuation of the measurements. The monthly distributions of CS, and SO_2 and NO_x concentrations could be represented by constant values of the overall means and SDs of $(9.4\pm4.3)\times10^{-3}$ s^{-1}, 4.7±2.1 µg m^{-3} and 81±38 µg m^{-3}, respectively with an acceptable accuracy. This suggests that CS, SO_2 and NO_x in Budapest do not critically or substantially affect either the dynamic properties (or the event occurrence). Monthly distributions of air T and O_3 concentration showed a maximum over summer months, while RH reflected the T tendency. Distribution of CO was more changing and less certain than for the other gases, and, therefore, its interpretation is encumbered so far. However, it doesn't seem to obviously affect the dynamic properties.

Atmos. Chem. Phys. Discuss., https://doi.org/10.5194/acp-2018-918
Manuscript under review for journal Atmos. Chem. Phys.
Discussion started: 1 October 2018

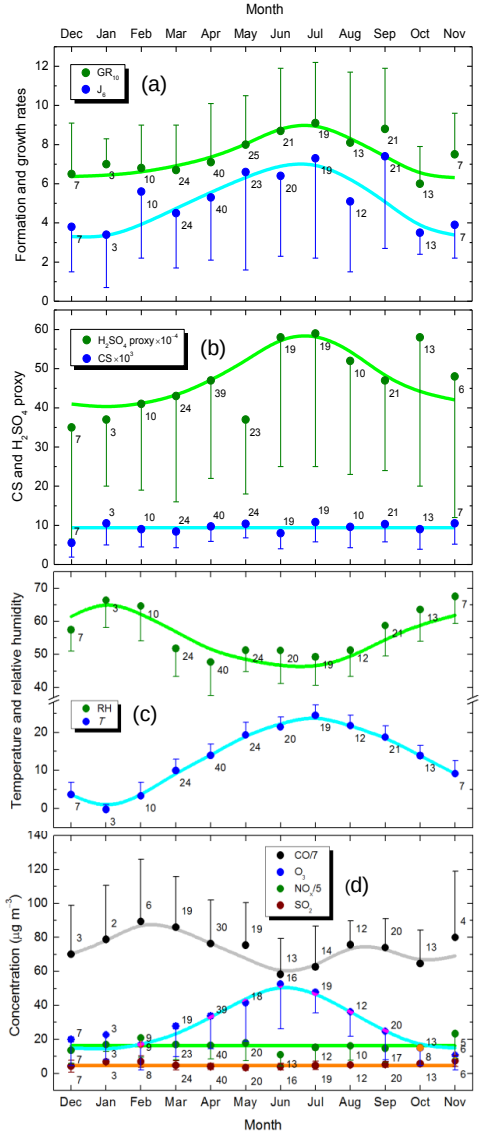

Figure 2. Distribution of monthly mean aerosol particle formation rate J_6 in a unit of cm^{-3} s^{-1} and particle diameter growth rate GR_{10} in a unit of nm h^{-1} (a), mean condensation sink for vapours (CS) in a unit of s^{-1} averaged over the nucleation time interval (t_1, t_2) and daily maximum gas-phase H_2SO_4 proxy in a unit of μg m^{-5} W s (b), daily mean air temperature (T) in a unit of °C and daily mean relative humidity (RH) in % (c), and daily median concentrations of SO_2, O_3, NO_x and CO for quantifiable (class 1A) new particle formation and growth events in the city centre for the joint 5-year long time interval. The error bars are shown for one side for clarity, and indicate 1 standard deviation. Number of the individual data averaged in each month is displayed next to the symbols. The horizontal lines indicate the overall mean. The nonlinear curves assist to guide the eye.

538 **4.3 Relationships**

539

540 Pearson's coefficients of correlation (R) between J_6 and GR_{10} revealed significant linear
541 relationship between them for all annual data sets (the mean R and SD were 0.768±0.099,
542 number of data pairs n=243). It has to be noted that J_6 and GR_{10} are not completely independent
543 variables (see Eq. 1 and Table S1). Scatter plots between J_6 and GR_{10} for the separate 1-year
544 long measurement time intervals are shown in Fig. 3. For the city centre, the regression lines
545 follow the line of equality in all 5 years. The mean slope (b) with SD for the joint 5-year long
546 city centre data set was b=0.94±0.07 expressed formally in a unit of cm^{-3} s^{-1} nm^{-1} h. At the
547 same time, the regression line for the near-city background deviated significantly from the
548 J_6=GR_{10} line, with a b=0.67±0.10 cm^{-3} s^{-1} nm^{-1} h. This implies that the relevant chemical
549 species and/or their processes in the air of the city centre contribute equally to the formation of
550 6-nm particles and to their growth process. In the near-city background, however, the chemical
551 compounds available and their processes power particle growth more than new particle
552 formation. This may be related to the differences between the city and its close environments
553 as far as the atmospheric composition, chemistry and physics, and other delicate conditions are
554 concerned (Paasonen et al., 2018). The narrower range and smaller number of individual
555 dynamic properties available in the near-city background relative to those in the city centre may
556 represent some weakness in the explanation. The intercepts (a) of the regression lines were,
557 however, identical for all data sets within their uncertainty interval. The mean intercept and SD
558 were estimated to be –1.7±0.8 cm^{-3} s^{-1}. This finding is interpreted as the existence of a
559 minimum GR or more exactly of a minimally required GR that corresponds to J_6=0. Particles
560 that exhibit at least this level of GR can escape coagulation mainly with larger particles, and
561 reach the diameter of 6 nm detectable in the present study by condensational growth. The
562 minimal GR was derived as GR_{min}= $-a/b$, and its mean and SD are 1.8±1.0 nm h^{-1} for the
563 conditions ordinarily present in the Budapest air. Nucleation processes which are initiated under
564 circumstances that cause the newly formed particle with a diameter of 10 nm to grow with a
565 rate <GR_{min} are normally not observed. Anyway, these are expected to be weak phenomena due
566 to the relationship between GR_{10} and J_6, while the events close to it can also be masked by
567 fluctuating experimental data. Their identification and evaluation can be made feasible by
568 decreasing the lower measurement diameter limit of DMPS systems down to 3 nm, or by
569 different instruments such as particle size magnifier or neutral cluster and air ions spectrometer.
570

Atmos. Chem. Phys. Discuss., https://doi.org/10.5194/acp-2018-918
Manuscript under review for journal Atmos. Chem. Phys.
Discussion started: 1 October 2018

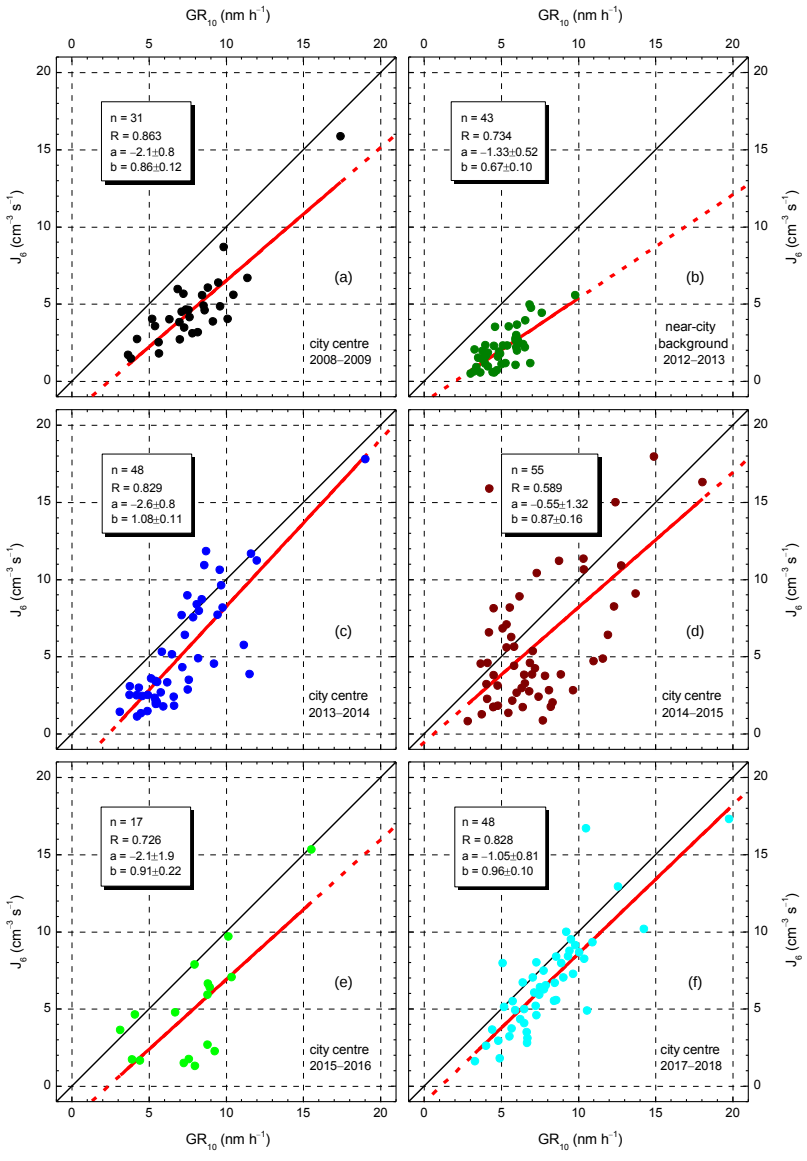

Figure 3. Scatter plots for aerosol particle formation rate J_6 and consecutive particle diameter growth rate GR_{10} in city centre (a and c–f) and near-city background (b) separately for the 1-year long measurement time intervals. Number of data point (*n*), their coefficient of correlation (*R*) and the intercept (*a*) and slope (*b*) of the regression line with standard deviations are also indicated. The lines in black represent the line of equality J_6=GR_{10}, the solid lines in red show the regression lines, while the dashed parts in red are extrapolated from the regression line.

Correlations between individual H_2SO_4 proxy values on one side and J_6 or GR_{10} on the other side were not significant. This is consistent with the corresponding conclusion of Sect. 4.2 and with the earlier results according to which the mean contribution of H_2SO_4 condensation to the particle GR was only 12.3% in Budapest (Salma et al., 2016b). The lack of correlation repeatedly suggests that other chemical species have larger influence on the formation and growth of new particles. Coefficients of correlation between CS on one side and J_6 or GR_{10} on the other side for the joint city centre data sets were modest (R=0.41 and 0.32, respectively with n=194 and 197, respectively). This is simply related to the fact that larger GR values are typical for polluted urban air (Kulmala et al., 2017) since particles capable of escaping coagulation scavenging need to grow faster in comparison to cleaner environments, and the enhanced requirements for the growth are linked to increased formation rates as well. As far as the pollutant gases are concerned, no correlation could be identified between J_6 or GR_{10} on one side and the gas concentrations on the other side. The coefficients of correlation between CS and NO_x or CO were modest (R=0.37 and 0.42, respectively with n=164 and 152, respectively), while correlation of NO_x and CO on one side with WS was also modest but negative (R= –0.32 and –0.42, respectively with n=167 and 155, respectively). The former relationships can be explained by the fact that vehicular road traffic in cities is a considerable common sources of NO_x, CO and primary particles (Paasonen et al., 2016), and the emitted particles largely contribute to CS levels, while the latter relationships are linked to the effect of large-scale air mass transport (often connected to high WSs) on urban air pollution or air quality.

Importance and contribution of condensing vapours other than H_2SO_4 are further demonstrated in Fig. 4. The data for the city centre and near-city background were presented in a linearized form and separately for the 2 sites. Nevertheless, the fitting of the correlation line was accomplished for the joint 6-year long data set. It can be demonstrated in particular on non-linearized plot of the GR_{10}/H_2SO_4 proxy as function of H_2SO_4 proxy (not shown here) that the 2 data sets merge into each other without any relevant structure, and, therefore, that they can be regarded to be coherent. This approach seems sensible when considering also the limited accuracy of the values. The relationship between the 2 composite variables in Fig. 4 was significant (R^2=0.800, p<0.05). It can be interpreted as the increasing atmospheric concentration of gas-phase H_2SO_4 can be related to larger contributions of other vapours than H_2SO_4 to particle growth. The other or competing compounds may include oxidation products and their dimers from photooxidation of VOC precursors from both biogenic and anthropogenic sources.

Atmos. Chem. Phys. Discuss., https://doi.org/10.5194/acp-2018-918
Manuscript under review for journal Atmos. Chem. Phys.
Discussion started: 1 October 2018

Atmospheric Chemistry and Physics Discussions

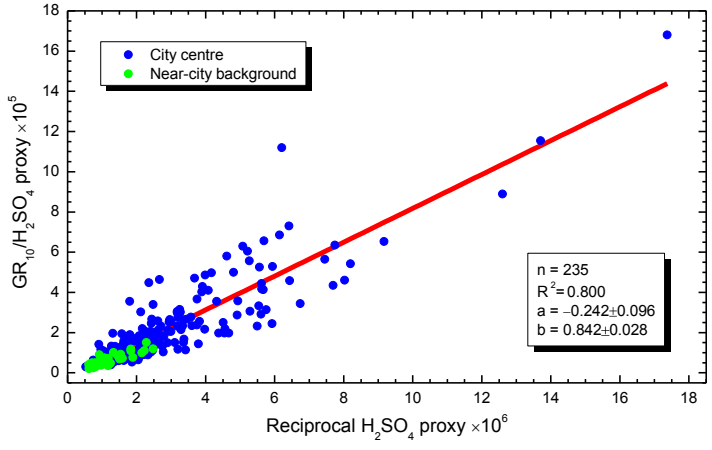

Figure 4. Dependence of the growth rate GR_{10} (in a unit of nm h^{-1}) of new particle formation and growth events normalised to the daily maximum gas-phase H_2SO_4 proxy (μg m^{-5} W s) on the reciprocal proxy value in the city centre and near-city background. The linear line in red represents the line fitted to the joint data set. Number of individual data considered (*n*), their coefficient of determination (R^2) and the intercept (*a*) and slope (*b*) of the fitted regression line with standard deviations are also shown.

4.4 Extreme and multiple events

The joint 6-year long data sets of J_6, GR_{10} and Δt containing all, 247 individual data each could be characterised by lognormal distribution function. This is demonstrated by log-probability graph for J_6 in Fig. S2 as example. The coefficient of determination, median and geometric standard deviation for J_6, GR_{10} and Δt data sets were 0.990, 4.0 cm^{-3} and 2.3; 0.993, 6.8 nm h^{-1} and 1.46; and 0.998, 02:57 (0.123 d) and 1.74, respectively. One of the major properties of this distribution type is that it contains relatively large individual data with considerably high abundances. There were 5 individual J_6 and 5 individual GR_{10} data above the 98% percentile of the data sets, which belonged to 9 separate NPF and growth events (days). Their specifications, properties and parameters are summarised in Table 3. All these events occurred in the city centre from April to September. Their number in the separate consecutive measurement years (Sect. 2) were 1, 0, 1, 2, 0 and 5, respectively. The medians of J_6, GR_{10}, CS and air *T* for the subsets of these 9 extreme event days were larger by factors of 5.2, 2.4, 1.5 and 1.4, respectively than for the city centre data, while the medians of the other properties and concentrations in these 2 respective data sets agreed within approximately 10%. There was a single event associated with an extreme H_2SO_4 proxy (of 23×10^{-5} μg m^{-5} W s) and relatively

Atmos. Chem. Phys. Discuss., https://doi.org/10.5194/acp-2018-918
Manuscript under review for journal Atmos. Chem. Phys.
Discussion started: 1 October 2018

Atmospheric Chemistry and Physics Discussions

low NO_x concentration (44 µg m^{-3}), which indicate exceptionally favourable conditions for NPF and growth. In addition to this case, there were only a few (1–2) days that were characterised by an unusually large CS (23×10^{-3} s^{-1}) – which could in turn be linked to higher dynamic rates (Sect. 4.3) – or by somewhat larger SO_2 (8.1 µg m^{-3}) or lower NO_x concentration (34 µg m^{-3}). For all the other events, however, no simple or compound property of the investigated variables could explain the extreme rates. Instead, they may be related to some other chemical species and/or atmospheric processes, which were not including in the present study. Since the extreme NPF and growth events usually resembled the time evolution for regional events (well developed banana curves) – sometimes with multiple onsets –, the missing atmospheric players in increased concentrations or their relevant processes are expected to appear on a larger horizontal spatial scale.

Table 3. Date (in a format of dd–MM–yyyy), new particle formation rate J_6 (in a unit of cm^{-3} s^{-1}), particle diameter growth rate GR_{10} (nm h^{-1}), starting time t_1 of nucleation (HH:mm UTC+1), duration time interval $\Delta t=t_2-t_1$ of nucleation (HH:mm), mean condensation sink CS during the nucleation process (10^{-3} s^{-1}), daily maximum gas-phase H_2SO_4 proxy (10^4 µg m^{-5} W s), daily mean air temperature T (°C), daily mean relative humidity RH (%), daily median concentrations of SO_2, O_3, NO_x (µg m^{-3}) and CO (mg m^{-3}) gases, and the type of the onset for extreme quantifiable (class 1A) new particle formation and growth events. The cells in yellow indicate the values which are above the 98% percentile of the corresponding data sets. N.a.: not available.

Date/ property	15–09–2009	20–04–2014	19–05–2015	04–07–2015	28–05–2017	25–06–2017	02–08–2017	31–08–2017	09–09–2017
J_6	15.9	17.8	24	16.3	27	33	30	47	17.3
GR_{10}	17.4	19.0	12.2	18.0	9.2	17.0	11.8	21	19.8
t_1	10:20	08:52	08:52	09:38	06:34	10:18	07:39	10:06	11:38
Δt	01:23	01:42	03:57	02:06	07:15	02:46	06:58	06:19	02:06
Proxy	38	42	25	16	229	41	69	92	45
CS	13.4	8.9	13.7	11.9	6.9	10.5	23	18.2	15.5
T	20	13.0	22	26	20	24	29	23	19.1
RH	60	62	48	40	40	68	49	47	58
SO_2	6.1	2.5	4.4	2.3	3.4	3.1	5.6	8.1	6.6
O_3	16.3	43	n.a.	33	61	56	34	24	12.9
NO_x	69	34	174	70	44	66	n.a.	109	112
CO	0.42	n.a.	0.71	0.33	0.31	0.50	0.97	0.62	0.71
Onset	ordinary	double	broad	ordinary	broad	broad	broad	broad	ordinary

Each quantifiable NPF and growth event was labelled as ordinary or broad by visual inspection of its beginning part. If the width of the beginning was smaller than approximately 2 h or there was a determinant single growth curve (rib) on the size distribution surface plot then the onset was labelled as ordinary, otherwise as broad (Fig. S1a and S1c for broad onsets). Broad onsets can be generated by 1) long-lasting nucleation process, 2) disrupted and started over nucleation due to changing atmospheric and meteorological conditions or 3) multiple nucleation processes close to each other in time (Salma et al., 2016b). The broad onsets were specified as doublets if the nucleation mode could be separated into 2 submodes by size distribution fitting. Approximately 40% of all quantifiable events had a broad onset. This indicates that NPF and growth events with broad/multiple onsets are abundant in the urban environment. This could be an important difference from remote or clean atmospheres. For 9% of all cases, it was feasible to calculate 2 sets of dynamic properties for onsets 1 and 2, respectively with a reasonable accuracy. In the near-city background, the medians of J_6 and GR_{10} for the onset 1 were similar or somewhat smaller than the corresponding medians for the whole near-city background data set, while for the onset 2, they were substantially larger, namely 4.1 cm^{-3} s^{-1} and 10.0 nm h^{-1}, respectively (cf. Table 2). Actually, the latter values were closer to the medians of the city centre than for the near-city background. The dynamic properties for the city centre for both the onset 1 and onset 2 were somewhat larger than for the whole the city centre data set. Approximately 75% of the doublets resulted in individual onset2/onset1 ratios larger than unity. Their overall median ratios for J_6 and GR_{10} were similar and approximately 1.4, while for the near-city background, they were about 2. The results are in line with and confirm our earlier conclusion according to which the second onsets (if it is a new formation process and not just a started over event) often generate new particles more intensively than the first onsets (Salma et al., 2016b). These particles also grow faster. This can be explained by the fact that the first event is often or likely of regional scale since its dynamic properties resemble those of the regional background process (Yli-Juuti et al., 2009), while the later event can be characterised by values typical for the city centre (Salma et al., 2016b). The later event (or events) are mainly caused and governed by sub-regional processes. These findings are also coherent with a previous observation of NPF and growth events with multiple onsets in semi-clean savannah and industrial environments (Hirsikko et al., 2013), and they also fit well into the existing ideas on mixing regional and urban air parcels that exhibit different properties such as precursor concentrations, T and RH (Kulmala et al., 2017).

5 Conclusions

Dynamic and timing properties of 247 NPF and growth events were studied together with supporting aerosol properties, meteorological data and pollutant gas concentrations in near-city background and city centre of Budapest for 6 years. The results and conclusions derived here can form in important component that is based on atmospheric observations, and is to be combine with results from laboratory experiments and finally, with theoretical models to further improve our understanding on the NPF potentials to increase UF and CCN concentrations on various spatial and temporal scales. Magnitude of the particle number concentration level produced solely by NPF and growth (strength of the events) can roughly be estimated by considering the median J_6, median duration of the nucleation process (Table 2) and the typical coagulation loss of these particles (0.17; Sect. 3.1 and Table S1). In central Budapest, it yields a concentration of 10^4 cm^{-3}, which is comparable to the annual median concentrations (Sect. 4). This simple example indicates that the phenomenon is not only relevant for aerosol load and climate issues on larger/regional or global spatial scales (which were first recognised) but it can affect the urban climate and the health risk of inhabitants of cities as well. This recognition lead to emergence of the urban studies. At present, there is an evident and strong need for continuous urban NPF and growth studies on long term at fixed locations including relevant precursors and potential chemical participants of the phenomenon. They can also contribute to our general understanding of the nucleation phenomenon when their specialities and peculiarities are resolved and taken into account when dealing with its various implications.

The present research based on ambient atmospheric measurements provided several evidence that some important chemical players in the NPF and growth events are still missing. Considering the results and conclusions of cloud chamber experiments, these factors are expected to be related mainly to oxidation products of VOCs and/or their processes. Further dedicated research including sophisticated measurements, data evaluations and modelling studies is required to find and identify these species and their processes, and to account their multifactorial role in more detail. Such measurement campaign focusing on chemical composition of molecular clusters, precursors and nucleating vapours by applying recent expedient instruments in Budapest over the months of the highest expected event occurrence has been just realised within a frame of an international cooperation. Its perspective results can hopefully provide additional and valuable information for some of the conclusion base on indirect evidence so far, and can further clarify the overall picture on urban multicomponent nucleation and growth phenomenon.

762 **Data availability.** The observational data used in this paper are available on request from the
763 corresponding author or at the website of the Budapest platform for Aerosol Research and Training
764 (http://salma.web.elte.hu/BpART).

765 **Competing interest.** The authors declare that they have no conflict of interest.

766 **Acknowledgements.** The authors thank Markku Kulmala and his research team at the University of
767 Helsinki for their cooperation. Financial support by the National Research, Development and Innovation
768 Office, Hungary (contracts K116788 and PD124283); by the European Regional Development Fund
769 and the Hungarian Government (GINOP-2.3.2-15-2016-00028) is gratefully acknowledged.
770

771 **References**

772 Alam, A., Shi, J. P., and Harrison, R. M.: Observations of new particle formation in urban air, J.
773 Geophys. Res., 108 (D3), 4093, doi:10.1029/2001JD001417, 2003.
774 Almeida, J., Schobesberger, S., Kurten, A., Ortega, I. K., Kupiainen-Maatta, O., Praplan, A. P.,
775 Adamov, A., Amorim, A., Bianchi, F., Breitenlechner, M., David, A., Dommen, J., Donahue, N.
776 M., Downard, A., Dunne, E., Duplissy, J., Ehrhart, S., Flagan, R. C., Franchin, A., Guida, R.,
777 Hakala, J., Hansel, A., Heinritzi, M., Henschel, H., Jokinen, T., Junninen, H., Kajos, M.,
778 Kangasluoma, J., Keskinen, H., Kupc, A., Kurten, T., Kvashin, A. N., Laaksonen, A., Lehtipalo,
779 K., Leiminger, M., Leppa, J., Loukonen, V., Makhmutov, V., Mathot, S., McGrath, M. J.,
780 Nieminen, T., Olenius, T., Onnela, A., Petäjä, T., Riccobono, F., Riipinen, I., Rissanen, M., Rondo,
781 L., Ruuskanen, T., Santos, F. D., Sarnela, N., Schallhart, S., Schnitzhofer, R., Seinfeld, J. H.,
782 Simon, M., Sipilä, M., Stozhkov, Y., Stratmann, F., Tome, A., Tröstl, J., Tsagkogeorgas, G.,
783 Vaattovaara, P., Viisanen, Y., Virtanen, A., Vrtala, A., Wagner, P. E., Weingartner, E., Wex, H.,
784 Williamson, C., Wimmer, D., Ye, P. L., Yli-Juuti, T., Carslaw, K. S., Kulmala, M., Curtius, J.,
785 Baltensperger, U., Worsnop, D. R., Vehkamäki, H., and Kirkby, J.: Molecular understanding of
786 sulphuric acid–amine particle nucleation in the atmosphere, Nature, 502, 359–363, 2013.
787 Baltensperger, U., Streit, N., Weingartner, E., Nyeki, S., Prévôt, A. S. H., Van Dingenen, R., Virkkula,
788 A., Putaud, J. P., Even, A., Brink, H., Blatter, A., Neftel, A., and Gaggeler, H. W.: Urban and rural
789 aerosol characterization of summer smog events during the PIPAPO field campaign in Milan, Italy,
790 J. Geophys. Res., 107(D22), 8193, doi:10.1029/2001JD001292, 2002.
791 Bianchi, F., Tröstl, J., Junninen, H., Frege, C., Henne, S., Hoyle, C. R., Molteni, U., Herrmann, E.,
792 Adamov, A., Bukowiecki, N., Chen, X., Duplissy, J., Gysel, M., Hutterli, M. Kangasluoma, J.,
793 Kontkanen, J., Kürten, A. Manninen, H. E., Münch, S., Peräkylä, O., Petäjä, T., Rondo, L.,
794 Williamson, C., Weingartner, E. Curtius, J., Worsnop, D. R., Kulmala, M., Dommen, J., and
795 Baltensperger, U.: New particle formation in the free troposphere: A question of chemistry and
796 timing, Science, 352, 1109–1112, https://doi.org/10.1126/science.aad5456, 2016.
797 Braakhuis, H. M., Park, M. V., Gosens, I., De Jong, W. H., and Cassee, F. R.: Physicochemical
798 characteristics of nanomaterials that affect pulmonary inflammation, Part. Fibre Toxicol., 11:18,
799 doi: 10.1186/1743-8977-11-18, 2014.

800 Cai, R. and Jiang, J.: A new balance formula to estimate new particle formation rate: reevaluating the
801 effect of coagulation scavenging, Atmos. Chem. Phys., 17, 12659–12675, 2017.
802 Carslaw, K. S., Lee, L. A., Reddington, C. L., Pringle, K. J., Rap, A., Forster, P. M., Mann, G. W.,
803 Spracklen, D. V., Woodhouse, M. T., Regayre, L. A., and Pierce, J. R: Large contribution of
804 natural aerosols to uncertainty in indirect forcing, Nature, 503, 67–71, 2013.
805 Crounse, J. D., Nielsen, L. B., Jørgensen, S., Kjaergaard, H. G., and Wennberg, P. O.: Autoxidation of
806 organic compounds in the atmosphere, J. Phys. Chem. Lett., 4, 20, 3513–3520, 2013.
807 Dal Maso, M., Kulmala, M., Lehtinen, K. E. J., Mäkelä, J. M., Aalto, P. P., and O'Dowd, C.:
808 Condensation and coagulation sinks and formation of nucleation mode particles in coastal and
809 boreal forest boundary layers, J. Geophys. Res., 107(19D), 8097, 10.1029/2001jd001053, 2002.
810 Dal Maso, M., Kulmala, M., Riipinen, I., Wagner, R., Hussein, T., Aalto, P. P., and Lehtinen, K. E. J.:
811 Formation and growth of fresh atmospheric aerosols: eight years of aerosol size distribution data
812 from SMEAR II, Hyytiälä, Finland, Boreal Environ. Res., 10, 323–336, 2005.
813 Dall'Osto, M., Querol, X., Alastuey, A., O'Dowd, C., Harrison, R. M., Wenger, J., and Gómez-
814 Moreno, F. J.: On the spatial distribution and evolution of ultrafine particles in Barcelona, Atmos.
815 Chem. Phys., 13, 741–759, 2013.
816 Ehn, M., Thornton, J. A., Kleist, E., Sipilä, M., Junninen, H., Pullinen, I., Springer, M., Rubach, F.,
817 Tillmann, R., Lee, B., Lopez-Hilfiker, F., Andres, S., Acir, I. H., Rissanen, M., Jokinen, T.,
818 Schobesberger, S., Kangasluoma, J., Kontkanen, J., Nieminen, T., Kurten, T., Nielsen, L. B.,
819 Jorgensen, S., Kjaergaard, H. G., Canagaratna, M., Dal Maso, M., Berndt, T., Petäjä, T., Wahner,
820 A., Kerminen, V. M., Kulmala, M., Worsnop, D. R., Wildt, J., and Mentel, T. F.: A large source of
821 low-volatility secondary organic aerosol, Nature, 506, 476–479, 2014.
822 Gordon, H., Sengupta, K., Rap, A., Duplissy, J., Frege, C., Williamson, C., Heinritzi, M., Simon, M.,
823 Yan, C., Almeida, J., Tröstl, J., Nieminen, T., Ortega, I. K., Wagner, R., Dunne, E. M., Adamov,
824 A., Amorim, A., Bernhammer, A. K., Bianchi, F., Breitenlechner, M., Brilke, S., Chen, X., Craven,
825 J. S., Dias, A., Ehrhart, S., Fischer, L., Flagan, R. C., Franchin, A., Fuchs, C., Guida, R., Hakala, J.,
826 Hoyle, C. R., Jokinen, T., Junninen, H., Kangasluoma, J., Kim, J., Kirkby, J., Krapf, M., Kürten,
827 A., Laaksonen, A., Lehtipalo, K., Makhmutov, V., Mathot, S., Molteni, U., Monks, S. A., Onnela,
828 A., Peräkylä, O., Piel, F., Petäjä, T., Praplan, A. P., Pringle, K. J., Richards, N. A. D., Rissanen, M.
829 P., Rondo, L., Sarnela, N., Schobesberger, S., Scott, C. E., Seinfeld, J. H., Sharma, S., Sipilä, M.,
830 Steiner, G., Stozhkov, Y., Stratmann, F., Tomé, A., Virtanen, A., Vogel, A. L., Wagner, A. C.,
831 Wagner, P. E., Weingartner, E., Wimmer, D., Winkler, P. M., Ye, P., Zhang, X., Hansel, A.,
832 Dommen, J., Donahue, N. M., Worsnop, D. R., Baltensperger, U., Kulmala, M., Curtius, J., and
833 Carslaw, K. S.: Reduced anthropogenic aerosol radiative forcing caused by biogenic new particle
834 formation, Proc. Natl. Acad. Sci. U.S.A., 113, 12053–12058,
835 https://doi.org/10.1073/pnas.1602360113, 2016.
836 Hirsikko, A., Vakkari, V., Tiitta, P., Hatakka, J., Kerminen, V.-M., Sundström, A.-M., Beukes, J. P.,
837 Manninen, H. E., Kulmala, M., and Laakso, L.: Multiple daytime nucleation events in semi-clean
838 savannah and industrial environments in South Africa: analysis based on observations, Atmos.
839 Chem. Phys., 13, 5523–5532, 2013.

840 Hussein, T., Puustinen, A., Aalto, P. P., Mäkelä, J. M., Hämeri, K., and Kulmala, M.: Urban aerosol
841 number size distributions, Atmos. Chem. Phys., 4, 391–411, 2004.
842 Hussein, T., Martikainen, J., Junninen, H., Sogacheva, L., Wagner, R., Dal Maso, M., Riipinen, I.,
843 Aalto, P. P., and Kulmala, M.: Observation of regional new particle formation in the urban
844 atmosphere, Tellus 60B, 509–521, 2008.
845 Jokinen, T., Berndt, T., Makkonen, R., Kerminen, V.-M., Junninen, H., Paasonen, P., Stratmann, F.,
846 Herrmann, H., Guenther, A. B., Worsnop, D. R., Kulmala, M., Ehn, M. and Sipilä, M.: Production
847 of extremely low volatile organic compounds from biogenic emissions: Measured yields and
848 atmospheric implications, Proc. Natl. Acad. Sci. U.S.A., 112, 7123–7128, 2015.
849 Kerminen, V.-M., Paramonov, M., Anttila, T., Riipinen, I., Fountoukis, C., Korhonen, H., Asmi, E.,
850 Laakso, L., Lihavainen, H., Swietlicki, E., Svenningsson, B., Asmi, A., Pandis, S. N., Kulmala, M.,
851 and Petäjä, T.: Cloud condensation nuclei production associated with atmospheric nucleation: a
852 synthesis based on existing literature and new results, Atmos. Chem. Phys., 12, 12037–12059,
853 2012.
854 Kirkby, J., Curtius, J., Almeida, J., Dunne, E., Duplissy, J., Ehrhart, S., Franchin, A., Gagné, S., Ickes,
855 L., Kürten, A., Kupc, A., Metzger, A., Riccobono, F., Rondo, L., Schobesberger, S.,
856 Tsagkogeorgas, G., Wimmer, D., Amorim, A., Bianchi, F., Breitenlechner, M., David, A.,
857 Dommen, J., Downard, A., Ehn, M., Flagan, R. C., Haider, S., Hansel, A., Hauser, D., Jud, W.,
858 Junninen, H., Kreissl, F., Kvashin, A., Laaksonen, A., Lehtipalo, K., Lima, J., Lovejoy, E. R.,
859 Makhutov, V., Mathot, S., Mikkilä, J., Minginette, P., Mogo, S., Nieminen, T., Onnela, A., Pereira,
860 A., Petäjä, T., Schnitzhofer, R., Seinfeld, J. H., Sipilä, M., Stozhkov, Y., Stratmann, F., Tome, A.,
861 Vanhanen, J., Viisanen Y., Vrtala, A., Wagner, P.E., Walther, H., Weingartner, E., Wex, H.,
862 Winkler, P.M., Carslaw, K. S., Worsnop, D. R., Baltensperger, U., and Kulmala, M.: The role of
863 sulfuric acid, ammonia and galactic cosmic rays in atmospheric aerosol nucleation, Nature, 476,
864 429–433, 2011.
865 Kirkby, J., Duplissy, J., Sengupta, K., Frege, C., Gordon, H., Williamson, C., Heinritzi, M., Simon,
866 M., Yan, C., Almeida, J., Tröstl, J., Nieminen, T., Ortega, I. K., Wagner, R., Adamov, A., Amorim,
867 A., Bernhammer, A.-K., Bianchi, F., Breitenlechner, M., Brilke, S., Chen, X., Craven, J., Dias, A.,
868 Ehrhart, S., Flagan, R. C., Franchin, A., Fuchs, C., Guida, R., Hakala, J., Hoyle, C. R., Jokinen, T.,
869 Junninen, H., Kangasluoma, J., Kim, J., Krapf, M., Kürten, A., Laaksonen, A., Lehtipalo, K.,
870 Makhmutov, V., Mathot, S., Molteni, U., Onnela, A., Peräkylä, O., Piel, F., Petäjä, T., Praplan, A.
871 P., Pringle, K., Rap, A., Richards, N. A. D., Riipinen, I., Rissanen, M. P., Rondo, L., Sarnela, N.,
872 Schobesberger, S., Scott, C. E., Seinfeld, J. H., Sipilä, M., Steiner, G., Stozhkov, Y., Stratmann, F.,
873 Tomé, A., Virtanen, A., Vogel, A. L., Wagner, A., Wagner, P. E., Weingartner, E., Wimmer, D.,
874 Winkler, P. M., Ye, P., Zhang, X., Hansel, A., Dommen, J., Donahue, N. M., Worsnop, D. R.,
875 Baltensperger, U., Kulmala, M., Carslaw, K. S., and Curtius, J.: Ion-induced nucleation of pure
876 biogenic particles, Nature, 533, 521–526, https://doi.org/10.1038/nature17953, 2016.
877 Kulmala, M., Dal Maso, M., Mäkelä, J. M., Pirjola, L., Väkevä, M., Aalto, P., Miikkulainen, P.,
878 Hämeri, K., and O'Dowd, C. D.: On the formation, growth and composition of nucleation mode
879 particles, Tellus B53, 479–490, 2001.

880 Kulmala, M., Vehkamäki, H., Petäjä, T., Dal Maso, M., Lauri, A., Kerminen, V.-M., Birmili, W., and
881 McMurry, P.: Formation and growth rates of ultrafine atmospheric particles: a review of
882 observations, J. Aerosol Sci., 35, 143–176, 2004.
883 Kulmala, M., Petäjä, T., Nieminen, T., Sipilä, M., Manninen, H. E., Lehtipalo, K., Dal Maso, M.,
884 Aalto, P. P., Junninen, H., Paasonen, P., Riipinen, I., Lehtinen, K. E. J., Laaksonen, A., and
885 Kerminen, V.-M.: Measurement of the nucleation of atmospheric aerosol particles, Nat. Protoc., 7,
886 1651–1667, doi:10.1038/nprot.2012.091, 2012.
887 Kulmala, M., Kontkanen, J., Junninen, H., Lehtipalo, K., Manninen, H. E., Nieminen, T., Petäjä, T.,
888 Sipilä, M., Schobesberger, S., Rantala, P., Franchin, A., Jokinen, T., Järvinen, E., Äijälä, M.,
889 Kangasluoma, J., Hakala, J., Aalto, P.P., Paasonen, P., Mikkilä, J., Vanhanen, J., Aalto, J., Hakola,
890 H., Makkonen, U., Ruuskanen, T., Mauldin, R. L. III, Duplissy, J., Vehkamäki, H., Bäck, J.,
891 Kortelainen, A., Riipinen, I., Kurtén, T., Johnston, M. V., Smith, J. N., Ehn, M., Mentel, T. F.,
892 Lehtinen, K. E. J., Laaksonen, A., Kerminen, V.-M., and Worsnop, D. R.: Direct observations of
893 atmospheric aerosol nucleation, Science, 339, 943–946, 2013.
894 Kulmala, M., Petäjä, T., Ehn, M., Thornton, J., Sipilä, M., Worsnop, D. R., and Kerminen, V.-M.:
895 Chemistry of atmospheric nucleation: On the recent advances on precursor characterization and
896 atmospheric cluster composition in connection with atmospheric new particle formation, Annu.
897 Rev. Phys. Chem., 65, 21−37, 2014.
898 Kulmala, M., Kerminen, V. M., Petäjä, T., Ding, A. J., and Wang, L.: Atmospheric gas-to-particle
899 conversion: why NPF events are observed in megacities, Faraday Discuss.,
900 doi:10.1039/C6FD00257A, 2017.
901 Makkonen, R., Asmi, A., Korhonen, H., Kokkola, H., Järvenoja, S., Räisänen, P., Lehtinen, K. E. J.,
902 Laaksonen, A., Kerminen, V.-M., Järvinen, H., Lohmann, U., Bennartz, R., Feichter, J., and
903 Kulmala, M.: Sensitivity of aerosol concentrations and cloud properties to nucleation and
904 secondary organic distribution in ECHAM5-HAM global circulation model, Atmos. Chem. Phys.,
905 9, 1747–1766, 2009.
906 Makkonen, R., Asmi, A., Kerminen, V.-M., Boy, M., Arneth, A., Hari, P., and Kulmala, M.: Air
907 pollution control and decreasing new particle formation lead to strong climate warming, Atmos.
908 Chem. Phys., 12, 1515–1524, 2012.
909 Merikanto, J., Spracklen, D. V., Mann, G. W., Pickering, S. J., and Carslaw, K. S.: Impact of
910 nucleation on global CCN, Atmos. Chem. Phys., 9, 8601–8616, 2009.
911 Metzger, A., Verheggen, B., Dommen, J., Duplissy, J., Prévôt, A. S. H., Weingartner, E., Riipinen, I.,
912 Kulmala, M., Spracklen, D. V., Carslaw, K. S., and Baltensperger, U.: Evidence for the role of
913 organics in aerosol particle formation under atmospheric conditions, Proc. Natl. Acad. Sci. U. S.
914 A., 107, 6646–6651, 2010.
915 Németh, Z. and Salma, I.: Spatial extension of nucleating air masses in the Carpathian Basin, Atmos.
916 Chem. Phys., 14, 8841–8848, 2014.
917 Németh, Z., Rosati, B., Zíková, N., Salma, I., Bozó, L., Dameto de España, C., Schwarz, J., Ždímal,
918 V., and Wonaschütz, A.: Comparison of atmospheric new particle formation and growth events in
919 three Central European cities, Atmos. Environ., 178, 191–197, 2018.

Nieminen, T., Kerminen, V.-M., Petäjä, T., Aalto, P. P., Arshinov, M., Asmi, E., Baltensperger, U., Beddows, D. C. S., Beukes, J. P., Collins, D., Ding, A., Harrison, R. M., Henzing, B., Hooda, R., Hu, M., Hõrrak, U., Kivekäs, N., Komsaare, K., Krejčí, R., Kristensson, A., Laakso, L., Laaksonen, A., Leaitch, W. R., Lihavainen, H., Mihalopoulos, N., Németh, Z., Nie, W., O'Dowd, C., Salma, I., Sellegri, K., Svenningsson, B., Swietlicki, E., Tunved, P., Ulevicius, V., Vakkari, V., Vana, M., Wiedensohler, A., Wu, Z., Virtanen, A., and Kulmala, M.: Global analysis of continental boundary layer new particle formation based on long-term measurements, Atmos. Chem. Phys. Discuss., https://doi.org/10.5194/acp-2018-304, in review, 2018.

Oberdörster, G., Oberdörster, E., and Oberdörster, J.: Nanotoxicology: an emerging discipline evolving from studies of ultrafine particles, Environ. Health Perspect., 113, 823–839, 2005.

O'Dowd, C. D., Jimenez, J. L., Bahreini, R. Flagan, R. C., Seinfeld, J. H., Hämeri, K., Pirjola, L., Kulmala, M., Jennings, S. G., and Hoffmann, Th.: Marine aerosol formation from biogenic iodine emissions, Nature 417, 632–636, 2002.

Paasonen, P., Kupiainen, K., Klimont, Z., Visschedijk, A., Denier van der Gon, H. A. C., and Amann, M.: Continental anthropogenic primary particle number emissions, Atmos. Chem. Phys., 16, 6823–6840, 2016.

Paasonen, P., Peltola, M., Kontkanen, J., Junninen, H., Kerminen, V.-M., and Kulmala, M.: Comprehensive analysis of particle growth rates from nucleation mode to cloud condensation nuclei in Boreal forest, Atmos. Chem. Phys. Discuss., https://doi.org/10.5194/acp-2018-169, in review, 2018.

Petäjä, T., Mauldin, III, R. L., Kosciuch, E., McGrath, J., Nieminen, T., Paasonen, P., Boy, M., Adamov, A., Kotiaho, T., and Kulmala, M.: Sulfuric acid and OH concentrations in a boreal forest site, Atmos. Chem. Phys., 9, 7435–7448, 2009.

Putaud, J.-P., Van Dingenen, R., Alastuey, A., Bauer, H., Birmili, W., Cyrys, J., Flentje, H., Fuzzi, S., Gehrig, R., Hansson, H. C., Harrison, R. M., Herrmann, H., Hitzenberger, R., Hüglin, C., Jones, A.M., Kasper-Giebl, A., Kiss, G., Kousa, A., Kuhlbusch, T. A. J., Löschau, G., Maenhaut, W., Molnár, A., Moreno, T., Pekkanen, J., Perrino, C., Pitz, M., Puxbaum, H., Querol, X., Rodriguez, S., Salma, I., Schwarz, J., Smolík, J., Schneider, J., Spindler, G., ten Brink, H., Turšič, J., Viana, M., Wiedensohler, and A., Raes, F.: A European Aerosol Phenomenology - 3: physical and chemical characteristics of particulate matter from 60 rural, urban, and kerbside sites across Europe, Atmos. Environ., 44, 1308–1320, 2010.

Riccobono, F., Schobesberger, S., Scott, C., Dommen, J., Ortega, I., Rondo, L., Almeida, J., Amorim, A., Bianchi, F., Breitenlechner, M., David, A., Downard, A., Dunne, E., Duplissy, J., Ehrhart, S., Flagan, R., Franchin, A., Hansel, A., Junninen, H., Kajos, M., Keskinen, H., Kupc, A., Kurten, A., Kvashin, A., Laaksonen, A., Lehtipalo, K., Makhmutov, V., Mathot, S., Nieminen, T., Onnela, A., Petäjä, T., Praplan, A., Santos, F., Schallhart, S., Seinfeld, J., Sipila, M., Spracklen, D., Stozhkov, Y., Stratmann, F., Tome, A., Tsagkogeorgas, G., Vaattovaara, P., Viisanen, Y., Vrtala, A., Wagner, P., Weingartner, E., Wex, H., Wimmer, D., Carslaw, K., Curtius, J., Donahue, N., Kirkby, J., Kulmala, M., Worsnop, D., and Baltensperger, U.: Oxidation products of biogenic emissions contribute to nucleation of atmospheric particles, Science, 344, 717–721, 2014.

960 Riipinen, I., Pierce, J. R., Yli-Juuti, T., Nieminen, T., Häkkinen, S., Ehn, M., Junninen, H., Lehtipalo,
961 K., Petäjä, T., Slowik, J., Chang, R., Shantz, N. C., Abbatt, J., Leaitch, W. R., Kerminen, V.-M.,
962 Worsnop, D. R., Pandis, S. N., Donahue, N. M., and Kulmala, M.: Organic condensation: a vital
963 link connecting aerosol formation to cloud condensation nuclei (CCN) concentrations, Atmos.
964 Chem. Phys., 11, 3865–3878, 2011.
965 Salma, I., Borsós, T., Weidinger, T., Aalto, P., Hussein, T., Dal Maso, M., and Kulmala, M.:
966 Production, growth and properties of ultrafine atmospheric aerosol particles in an urban
967 environment, Atmos. Chem. Phys., 11, 1339–1353, 2011.
968 Salma, I., Borsós, T., Németh, Z., Weidinger, T., Aalto, T., and Kulmala, M.: Comparative study of
969 ultrafine atmospheric aerosol within a city, Atmos. Environ., 92, 154–161, 2014.
970 Salma, I., Füri, P., Németh, Z., Farkas, Á., Balásházy, I., Hofmann, W., and Farkas, Á.: Lung burden
971 and deposition distribution of inhaled atmospheric urban ultrafine particles as the first step in their
972 health risk assessment, Atmos. Environ., 104, 39–49, 2015.
973 Salma, I., Németh, Z., Weidinger, T., Kovács, B., and Kristóf, G.: Measurement, growth types and
974 shrinkage of newly formed aerosol particles at an urban research platform, Atmos. Chem. Phys.,
975 16, 7837–7851, 2016a.
976 Salma, I., Németh, Z., Kerminen, V. M., Aalto, P., Nieminen, T., Weidinger, T., Molnár, Á., Imre, K.,
977 and Kulmala, M.: Regional effect on urban atmospheric nucleation, Atmos. Chem. Phys., 16,
978 8715–8728, 2016b.
979 Salma, I., Varga, V., and Németh, Z.: Quantification of an atmospheric nucleation and growth process
980 as a single source of aerosol particles in a city, Atmos. Chem. Phys., 17, 15007–15017, 2017.
981 Schobesberger, S., Junninen, H., Bianchi, F., Lonn, G., Ehn, M., Lehtipalo, K., Dommen, J., Ehrhart,
982 S., Ortega, I. K., Franchin, A., Nieminen, T., Riccobono, F., Hutterli, M., Duplissy, J., Almeida, J.,
983 Amorim, A., Breitenlechner, M., Downard, A. J., Dunne, E. M., Flagan, R. C., Kajos, M.,
984 Keskinen, H., Kirkby, J., Kupc, A., Kurten, A., Kurten, T., Laaksonen, A., Mathot, S., Onnela, A.,
985 Praplan, A. P., Rondo, L., Santos, F. D., Schallhart, S., Schnitzhofer, R., Sipilä, M., Tome, A.,
986 Tsagkogeorgas, G., Vehkamäki, H., Wimmer, D., Baltensperger, U., Carslaw, K. S., Curtius, J.,
987 Hansel, A., Petäjä, T., Kulmala, M., Donahue, N. M., and Worsnop, D. R.: Molecular
988 understanding of atmospheric particle formation from sulfuric acid and large oxidized organic
989 molecules, Proc. Natl. Acad. Sci. U.S.A., 110, 17223–17228, 10.1073/pnas.1306973110, 2013.
990 Sihto, S.-L., Mikkilä, J., Vanhanen, J., Ehn, M., Liao, L., Lehtipalo, K., Aalto, P. P., Duplissy, J.,
991 Petäjä, T., Kerminen, V.-M., Boy, M., and Kulmala, M.: Seasonal variation of CCN concentrations
992 and aerosol activation properties in boreal forest, Atmos. Chem. Phys., 11, 13269–13285, 2011.
993 Sipilä, M., Berndt, T., Petäjä, T., Brus, D., Vanhanen, J., Stratmann, F., Patokoski, J., Mauldin, R. L.
994 3rd, Hyvärinen, A. P., Lihavainen, H., and Kulmala, M.: The role of sulfuric acid in atmospheric
995 nucleation, Science, 327(5970), 1243-6. doi: 10.1126/science.1180315, 2010.
996 Spracklen, D. V., Carslaw, K. S., Merikanto, J., Mann, G. W., Reddington, C. L., Pickering, S., Ogren,
997 J. A., Andrews, E., Baltensperger, U., Weingartner, E., Boy, M., Kulmala. M., Laakso, L.,
998 Lihavainen, H., Kivekäs, N., Komppula, M., Mihalopoulos, N., Kouvarakis, G., Jennings, S. G.,
999 O'Dowd, C., Birmili, W., Wiedensohler, A., Weller, R., Gras, J., Laj, P., Sellegri, K., Bonn, B.,

Krejčí, R., Laaksonen, A., Hamed, A., Minikin, A., Harrison, R. M., Talbot, R., and Sun, J.: The contribution of boundary layer nucleation events to total particle concentrations on regional and global scales, Atmos. Chem. Phys., 6, 5631–5648, 2006.

Tröstl, J., Chuang, W. K., Gordon, H., Heinritzi, M., Yan, C., Molteni, U., Ahlm, L., Frege, C., Bianchi, F., Wagner, R., Simon, M., Lehtipalo, K., Williamson, C., Craven, J. S., Duplissy, J., Adamov, A., Almeida, J., Bernhammer, A. K., Breitenlechner, M., Brilke, S., Dias, A., Ehrhart, S., Flagan, R. C., Franchin, A., Fuchs, C., Guida, R., Gysel, M., Hansel, A., Hoyle, C. R., Jokinen, T., Junninen, H., Kangasluoma, J., Keskinen, H., Kim, J., Krapf, M., Kürten, A., Laaksonen, A., Lawler, M., Leiminger, M., Mathot, S., Möhler, O., Nieminen, T., Onnela, A., Petäjä, T., Piel, F. M., Miettinen, P., Rissanen, M. P., Rondo, L., Sarnela, N., Schobesberger, S., Sengupta, K., Sipilä, M., Smith, J. N., Steiner, G., Tomè, A., Virtanen, A., Wagner, A. C., Weingartner, E., Wimmer, D., Winkler, P. M., Ye, P. L., Carslaw, K. S., Curtius, J., Dommen, J., Kirkby, J., Kulmala, M., Riipinen, I., Worsnop, D. R., Donahue, N. M., and Baltensperger, U.: The role of low-volatility organic compounds in initial particle growth in the atmosphere, Nature, 533, 527, 10.1038/nature18271, 2016.

Vuollekoski, H., Sihto, S.-L., Kerminen, V.-M., Kulmala, M., and Lehtinen, K. E. J.: A numerical comparison of different methods for determining the particle formation rate, Atmos. Chem. Phys., 12, 2289–2295, 2012.

Wehner, B., Wiedensohler, A., Tuch, T. M., Wu, Z. J., Hu, M., Slanina, J., and Kiang, C. S.: Variability of the aerosol number size distribution in Beijing, China: new particle formation, dust storms, and high continental background, Geophys. Res. Lett., 31, L22108, 2004.

Wiedensohler, A., Cheng, Y. F., Nowak, A., Wehner, B., Achtert, P., Berghof, M., Birmili, W., Wu, Z. J., Hu, M., Zhu, T., Takegawa, N., Kita, K., Kondo, Y., Lou, S. R., Hofzumahaus, A., Holland, F., Wahner, A., Gunthe, S. S., Rose, D., Su, H., and Pöschl, U.: Mobility particle size spectrometers: harmonization of technical standards and data structure to facilitate high quality long-term observations of atmospheric particle number size distributions, Atmos. Meas. Tech., 5, 657–685, 2012.

Woo, K. S., Chen, D. R., Pui, D. Y. H., and McMurry, P. H.: Measurement of Atlanta aerosol size distributions: observations of ultrafine particle events, Aerosol Sci. Technol., 34, 75–87, 2001.

Xiao, S., Wang, M. Y., Yao, L., Kulmala, M., Zhou, B., Yang, X., Chen, J. M., Wang, D. F., Fu, Q. Y., Worsnop, D. R., and Wang, L.: Strong atmospheric new particle formation in winter in urban Shanghai, China, Atmos. Chem. Phys., 15, 1769–1781, 2015.

Yli-Juuti, T., Riipinen, I., Aalto, P. P., Nieminen, T., Maenhaut, W., Janssens, I. A., Claeys, M., Salma, I., Ocskay, R., Hoffer, A., Imre, K., and Kulmala, M.: Characteristics of new particle formation events and cluster ions at K-puszta, Hungary. Boreal Environ. Res., 14, 683–698, 2009.

Zhang, R., Wang, G., Guo, S., Zamora, M. L., Ying, Q., Lin, Y., Wang, W., Hu, M., and Wang, Y.: Formation of urban fine particulate matter, Chem. Rev., 115, 3803−3855, 2015.